

PAPER • OPEN ACCESS

Corrosion of stainless steels in acidic, neutral and alkaline saline media: Electrochemical and microscopic analysis

To cite this article: Sahaja Seethammaraju and Murali Rangarajan 2019 *IOP Conf. Ser.: Mater. Sci. Eng.* **577** 012188

View the [article online](#) for updates and enhancements.

You may also like

- [High precision batch mode micro-electro-discharge machining of metal alloys using DRIE silicon as a cutting tool](#)
Tao Li, Qing Bai and Yogesh B Gianchandani
- [Low Cost Electrodes for Alkaline Water Electrolysis](#)
Hamid Zamanizadeh, Bruno Georges Pollet, Alejandro Oyarce et al.
- [Electrochemical and hot corrosion analysis of novel AlBeSiTiV light weight HEA coating on SS316](#)
S N Kishan, R Anoosa Sree, U V Akhil et al.

ECS
The
Electrochemical
Society
Advancing solid state &
electrochemical science & technology

DISCOVER
how sustainability
intersects with
electrochemistry & solid
state science research

Corrosion of stainless steels in acidic, neutral and alkaline saline media: Electrochemical and microscopic analysis

Sahaja Seethammaraju¹, Murali Rangarajan^{2,3*}

¹Department of Electronics and Communication Engineering, Amrita School of Engineering, Coimbatore, Amrita Vishwa Vidyapeetham, India

²Center of Excellence in Advanced Materials and Green Technologies, Amrita School of Engineering, Coimbatore, Amrita Vishwa Vidyapeetham, India

³Department of Chemical Engineering and Materials Science, Amrita School of Engineering, Coimbatore, Amrita Vishwa Vidyapeetham, India

*Corresponding author E-mail: r_murali@cb.amrita.edu

Abstract. This study presents how SS304 and SS316 corrode in saline media, including in the presence of acid and alkali, through an electrochemical and microscopic analysis. SS304 and SS316 samples were studied for their corrosion resistance in 1M NaCl, and in the presence of either 1M HCl or 1M NaOH. Potentiodynamic polarization studies were carried out to determine the corrosion potentials and currents. From the anodic polarization, regions corresponding to corrosion, passivation and transpassivation were identified. Samples were corroded at different anodic potentials corresponding to the different regimes and were analysed using scanning electron microscopy (SEM) and energy dispersive X-ray spectroscopy (EDX). In 1M NaCl medium, SS304 exhibits pitting and passivation whereas SS316 does not. Transpassivation occurs through intergranular corrosion that connects the different pits. Making the medium acidic results in much higher corrosion rates for both SS304 and SS316, but the corroded surfaces bear vastly different structures. SS304 surface forms deep pits with large intergranular cracks resembling chimney stacks. However, SS316 surfaces show dendritic morphologies of deposited corrosion products, further evidenced by a higher O/Fe ratio in EDX measurements. In alkaline media, SS304 shows evidence of pits on whose edges corrosion products are deposited while no significant pitting is seen with SS316.

Keywords: SS304, SS316, Saline medium, Corrosion, Potentiodynamic Polarization, Pitting, Intergranular Corrosion

1. Introduction

Stainless steel is one of the most commonly used engineering material. Its corrosion behaviour in saline media – neutral, acidic and alkaline – has attracted significant interest over a long period of time. Among the grades of stainless steel commonly used are SS304 and SS316, the latter for more corrosive media. It is well known that the presence of molybdenum in SS316 significantly enhances its corrosion resistance.

Corrosion is a major challenge for engineers because of its pervasiveness, ability to cause significant damage to engineering structures and products and significant, if underappreciated, costs. To illustrate, the estimated cost of corrosion in India is more than \$63 billion. Corrosion is an electrochemical



surface phenomenon where regions of surface act as anodes, losing metal atoms, with nearby regions acting as cathodes to receive the lost electrons through reduction reactions. Therefore, electrochemical characterization techniques such as potentiodynamic polarization have long been used in determining the corrosion rates and behaviour of engineering materials. Typically, there are regions of nonlinear (Butler-Volmer) behaviour, Tafel-behaviour, passivation and transpassivation in the anodic polarization curves. While these shed light on the corrosion phenomenon, it is also well understood that corrosion is not merely uniform degradation of a metal or alloy surface to its more stable forms but that localized corrosion such as pitting can cause catastrophic engineering failures even with a loss of < 2% of material [1]. Therefore, it is important to correlate the features of anodic polarization curves with the forms or mechanisms of corrosion.

Different studies have focused on various modifications of stainless steel and their effects on corrosion. For instance, effects of annealing and sensitization [2], alloying [3], coatings [4], additive manufacturing such as selective laser melting [5] on corrosion of stainless steels have been studied. Effects of temperature on the corrosion of SS316L in sulphuric acid medium has been explored by Ayu Arwati et al [6]. Studies have also focused on the forms of corrosion in stainless steel such as erosion-corrosion, pitting, crevice corrosion and stress corrosion cracking [7-10]. Though potentiodynamic polarization curves show specific features corresponding to localized corrosion, interpreting the form of corrosion and the mechanisms of corrosion is not a trivial task. An approach towards deciphering these is to carry out microscopic analysis of corroded samples. This is undertaken in the present study.

A recent review discusses how processing of stainless steel and the resultant nanocrystalline structure influences its corrosion properties [11]. Different manufacturing processes such as welding can affect the corrosion behaviour of stainless steel, which has also been reviewed [12]. Such studies show correlations between the forms of corrosion and the electrochemical studies such as potentiodynamic polarization, impedance spectroscopy and *in situ* techniques [13]. Thus, establishing correlations between the potentiodynamic polarization, corrosion forms and the mechanisms of initiation and propagation of corrosion is of significant interest.

This study aims to explore the corrosion of two of the commonly used stainless steels, namely, SS304 and SS316, in saline media (1M NaCl) and also in accelerated corrosion media containing 1M HCl or 1M NaOH with 1M NaCl. Based on the anodic polarization curves, different regions are identified. Chronoamperometry studies are then used to corrode the steel samples at the identified constant potentials. These corroded surfaces are then examined using scanning electron microscopy (SEM) and energy-dispersive X-ray spectroscopy (EDX). Taken together, an understanding is sought to be developed regarding the mechanisms of corrosion of the two steels in the different saline media.

2. Experimental Details

2.1 Materials

Stainless steel samples (SS304 and SS316) were procured locally (Coimbatore Metal Mart). Analytical grade sodium chloride, hydrochloric acid and sodium hydroxide were procured from Sigma and used without further processing. Distilled water was used throughout the studies.

2.2 Sample preparation and corrosion experiments

Before corrosion studies, the stainless steel samples were polished in different grades of emery paper, then on 0.01 μm alumina slurry to obtain a mirror finish. Then samples were then rinsed in distilled water. An area of 2 cm^2 was exposed for corrosion and the samples were immediately subject to potentiodynamic polarization studies. The samples were polarized $\pm 1\text{V}$ from their open circuit potentials at a scan rate of 10 mV/s. For examining the forms of corrosion, potentiostatic polarization (chronoamperometry) studies were carried out at potentials identified from the potentiodynamic polarization curves.

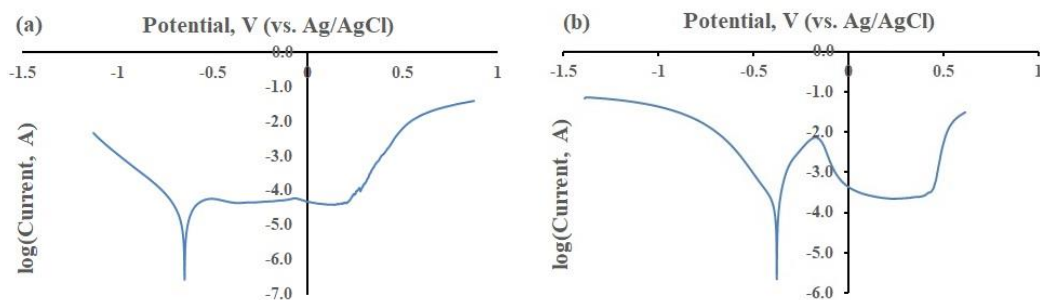
2.3 Characterization

Corroded samples were characterized for the surface morphology using a Carl Zeiss Field Emission Scanning Electron Microscope, with field emission gun operating at 10 kV. Energy Dispersive spectroscopy for obtaining the O/Fe ratio was carried out using Bruker attachment on SEM machine, EHT was set at 20 kV.

3. Results and discussions

Corrosion of SS304 and SS316 was studied using potentiodynamic polarization, scanning electron microscopy and energy dispersive X-ray spectroscopy (EDX). While it is well known that the corrosion resistance of SS304 is less than that of SS316 because of the presence of molybdenum, this study aims to shed light on the forms of corrosion of the stainless steels, the initiation and rates of those corrossions, and the effects of acidity and alkalinity (the addition of HCl and NaOH) on their corrosion.

Figures 1a-c show the potentiodynamic polarization curves of SS304 in 1M NaCl, 1M NaCl and 1M HCl, and 1M NaCl and 1M NaOH, respectively. The corresponding polarization curves for SS316 are presented in Figures 2a-c. The key differences between the corrosion of SS316 in NaCl vis-à-vis SS304 are clear upon comparing Figures 1a and 2a. The corrosion potentials and current densities are, SS304: $E_{\text{corr}} = -0.65\text{ V}$ and $I_{\text{corr}} = 1.009 \times 10^{-5}\text{ A/cm}^2$; SS316: $E_{\text{corr}} = -0.426\text{ V}$ and $I_{\text{corr}} = 2.499 \times 10^{-9}\text{ A/cm}^2$. There is a nearly four orders of magnitude reduction in corrosion current of SS316 compared to SS304. Further, it is seen that the initiation of corrosion in SS316 is shifted by about 220 mV.



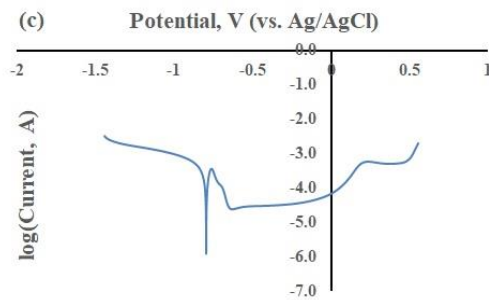


Figure 1. Potentiodynamic polarization of SS304 at a scan rate of 10 mV/s in (a) 1M NaCl, (b) 1M NaCl + 1M HCl, (c) 1M NaCl + 1M NaOH

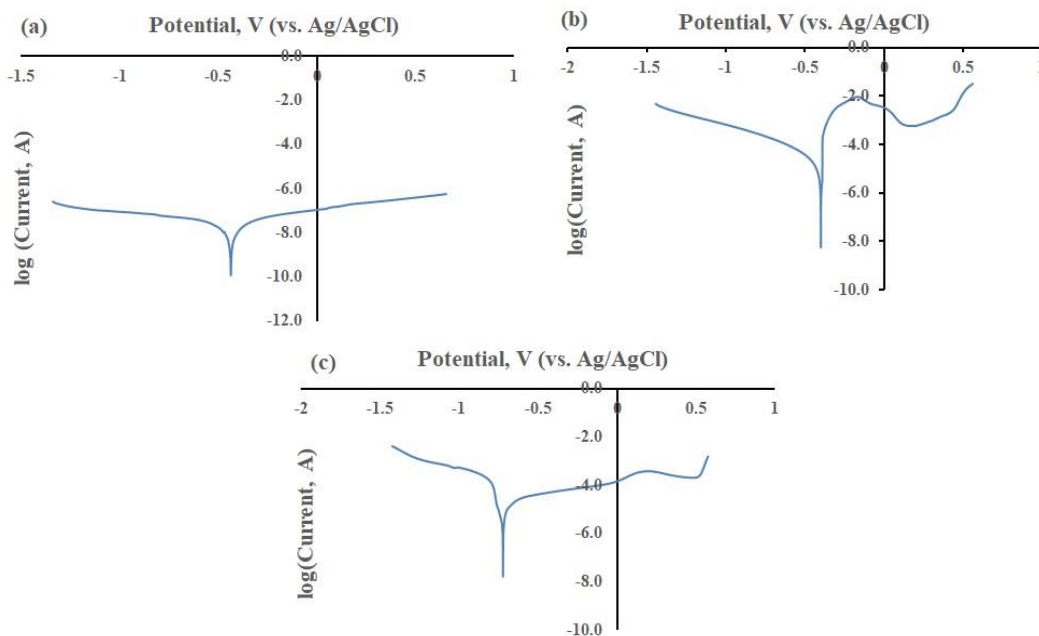


Figure 2. Potentiodynamic polarization of SS316 at a scan rate of 10 mV/s in (a) 1M NaCl, (b) 1M NaCl + 1M HCl, (c) 1M NaCl + 1M NaOH

Comparing the anodic polarization of SS304 and SS316 (right side of Figures 1a and 2a, respectively) reveals further important differences. SS304 passivates in NaCl, with passivation initiating at -0.5 V, with a constant current density of 2.26×10^{-5} A/cm², and then the passivation gives way to transpassivation at 0.202 V. However, SS316 shows no such feature in the potentiodynamic polarization curve. In order to further understand this, scanning electron microscopy was employed and the results are shown in Figures 3a-d and 4a-d. Figures 3a-b and 4a-b show, respectively, the SS304 and SS316 surfaces that have been corroded by 1M NaCl medium for 30 minutes at a potential of 0.1 V (by a chronoamperometry study, initiated from open circuit potential). It may be noted that this potential corresponds to the passivation region of the anodic polarization of SS304 in Figure 1a. In SS304 (Figure 3a), it is seen that pits are formed even at 0.1 V. Some of the surface defects are the residual defects in the samples (as they would be in commercially used steels). However, there are some new (small) pits that have been initiated. Further, the existing defects become deep pits, as seen

in Figure 3b. In contrast, SS316 shows no noticeable pits (Figures 4a and 4b). EDX spectra were used to determine the O/Fe ratio in the above samples. For SS304, this ratio was 0.012 whereas for SS316 it was 0.028. This further confirms the observation on SEM images that the corrosion products of SS316 (typically hydroxides) are deposited on the surface, resulting in higher oxygen content at the surface, whereas there are pits formed with lesser corrosion products on the surface in the case of SS304.

To better understand passivation and transpassivation processes from a microscopic analysis, fresh SS304 and SS316 samples were corroded first at 0.1 V (initiated from open circuit potential, to ensure passivation) and then at 0.4 V (from 0.1 V) for 30 minutes. In SS304 samples (Figures 3c and 3d), the pits are larger, and they spread through aligned intergranular corrosion that connect the different pits. On the other hand, in SS316 samples (Figure 4c and 4d), a similar behavior of existing defects being enlarged by corrosion is observed. However, corrosion products are deposited onto the surface, as is

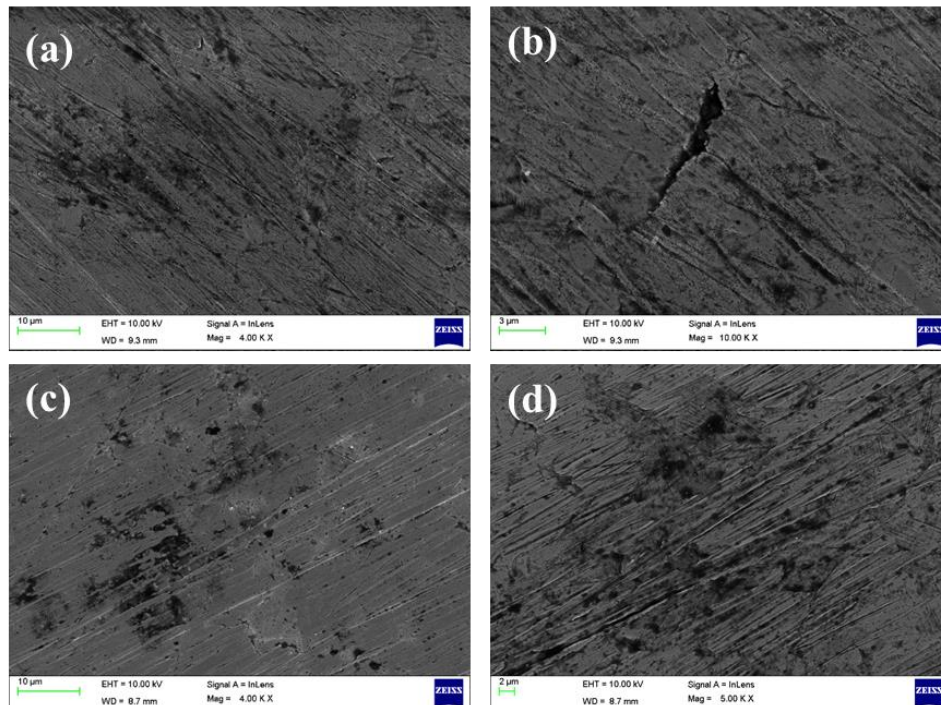


Figure 3. Scanning electron microscopy images of SS304 corroded in 1M NaCl for 30 minutes at (a, b) 0.1V, (c, d) 0.4V

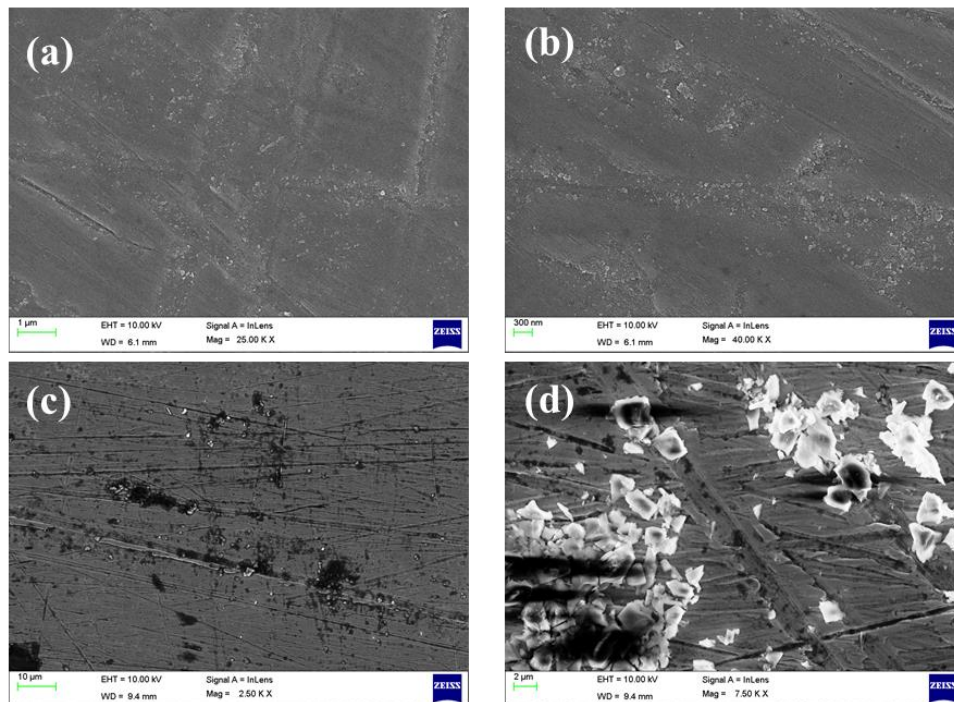


Figure 4. Scanning electron microscopy images of SS316 corroded in 1M NaCl for 30 minutes at (a, b) 0.1V, (c, d) 0.4V

particularly evident in Figure 4d. An analysis of the O/Fe ratio from EDX spectra revealed that SS304 had negligible oxygen atoms on the surface while the SS316 sample had an O/Fe ratio of 0.015. This is in line with the results obtained for corrosion at 0.1 V. Thus, it may be concluded that transpassivation occurs for SS304 samples by corrosion initiating from local pits in the form of intergranular corrosion, causing further dissolution.

Accelerated corrosion studies were carried out in the presence of either 1M HCl or 1M NaOH for both SS304 and SS316. In the presence of 1M NaCl and 1M HCl, the potentiodynamic polarization results are shown in Figures 1b and 2b, respectively. The corresponding corrosion potentials and current densities are, SS304: $E_{\text{corr}} = -0.382$ V and $I_{\text{corr}} = 7.84 \times 10^{-5}$ A/cm²; SS316: $E_{\text{corr}} = -0.39$ V and $I_{\text{corr}} = 4.562 \times 10^{-6}$ A/cm². In the acidic medium, the corrosion potentials are shifted for both SS304 and SS316 by 268 mV and 36 mV, respectively, and they begin corroding at similar potentials. The corrosion current density of SS316 is still 94% lesser than that of SS304.

The anodic polarization curves of SS304 and SS316 show significant differences. SS304 shows significant passivation, initiating at -0.156 V resulting in a nearly constant current of 1.104×10^{-4} A/cm². Transpassivation initiates at 0.43 V. SS316 shows similar passivation and transpassivation features. However, passivation initiates at -0.146 V and results in a minimum current of 2.951×10^{-4} A/cm². Transpassivation initiates at 0.212 V and further accelerates beyond 0.41 V. Scanning electron microscopy analyses were carried out on samples of SS304 and SS316 corroded in a medium containing 1M NaCl and 1M HCl for 30 minutes. Figures 5 and 6 present these results. For SS304 (Figure 5a-b), a sample was corroded at 0.25 V for 30 minutes while a SS316 sample (Figure 6a-b) was corroded at 0.15 V for 30 minutes. For the two steel samples, the corrosion currents may be

similar, but the surfaces are starkly different. For SS304 at 0.25 V (Figure 5a-b), large pits are formed with intergranular corroded regions connecting them. The pits resemble chimney stacks, with significant corrosion having occurred. SS316 (Figure 6a-b) does not show such strong pitting. Dendritic morphologies of corrosion products are coated with good surface coverage. The comparison of the O/Fe ratios for SS304 (0.092) and SS316 (0.160) reveal further how the corrosion products are better deposited on the surface for SS316, retarding further corrosion.

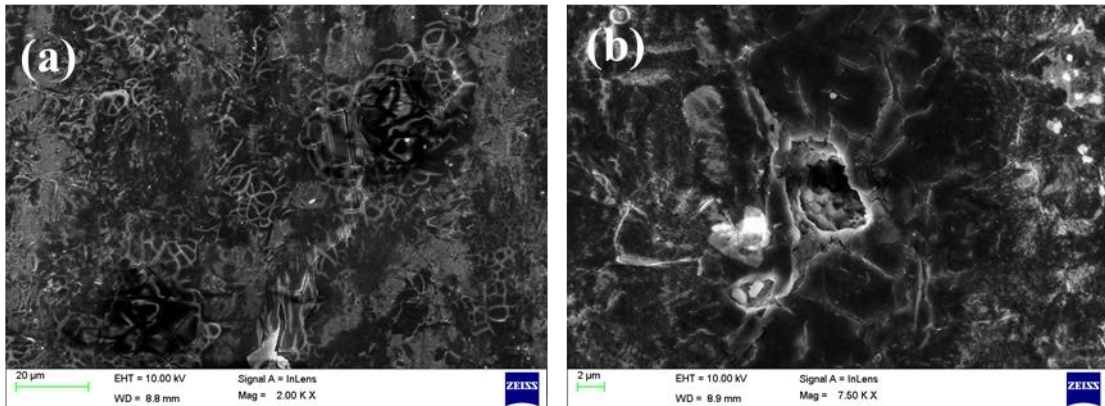


Figure 5. Scanning electron microscopy images of SS304 corroded in 1M NaCl and 1M HCl for 30 minutes at 0.25V

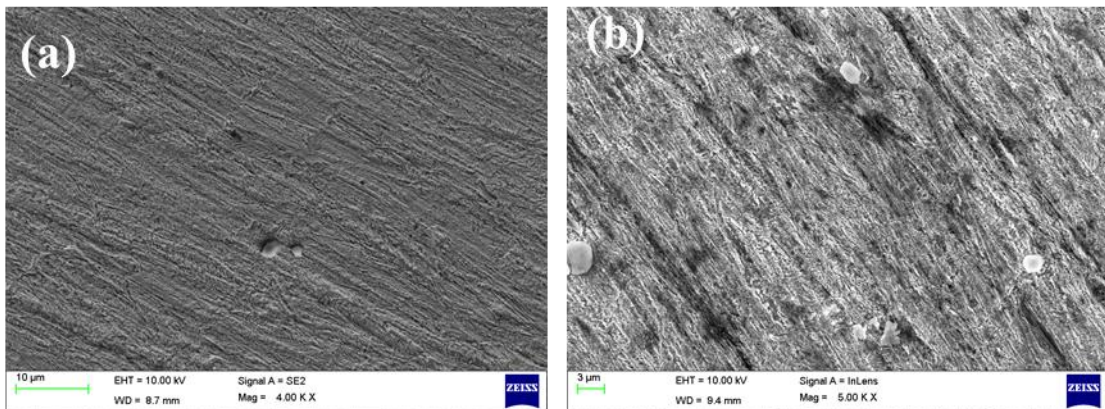


Figure 6. Scanning electron microscopy images of SS304 corroded in 1M NaCl and 1M HCl for 30 minutes at 0.15V

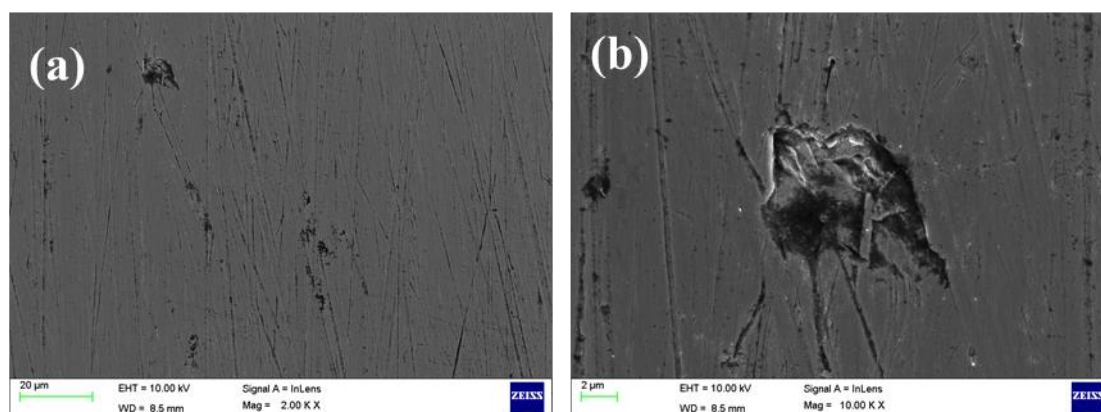


Figure 7. Scanning electron microscopy images of SS304 corroded in 1M NaCl and 1M NaOH for 30 minutes at 0.1V

When the steel samples were corroded in 1M NaCl and 1M NaOH media, the resultant potentiodynamic polarization curves showed similar comparisons, as depicted in Figures 1c and 2c, respectively, for SS304 and SS316. The corresponding corrosion potentials and current densities are, SS304: $E_{\text{corr}} = -0.797 \text{ V}$ and $I_{\text{corr}} = 1.682 \times 10^{-4} \text{ A/cm}^2$; SS316: $E_{\text{corr}} = -0.74 \text{ V}$ and $I_{\text{corr}} = 2.579 \times 10^{-6} \text{ A/cm}^2$. In the alkaline medium, the corrosion potentials are shifted for both SS304 and SS316 by -147 mV and -314 mV , respectively. The corrosion current density of SS316 is more than 98% lesser than that of SS304. For the SS304 sample, passivation initiates almost immediately after anodic polarization, at -0.756 V , while for the SS316 sample, passivation initiates at 0.225 V . Scanning electron microscopy studies were carried out on steel samples corroded in 1M NaCl and 1M NaOH media for 30 minutes. SS304 samples were corroded at 0.1 V for 30 minutes (Figure 7a-b), depicting pits formed in existing defects. The pit edges, brighter in color, are where the corrosion products are deposited. This potential corresponds to the first transpassivation region in the anodic polarization study (Figure 1c). When corroded at more anodic potentials (0.4 V), there were no new features observed except the deepening of the corrosion along existing defects (images not shown). SS316 samples were corroded at 0.2 V for 30 minutes, corresponding to the passivation region of the anodic polarization curve (Figure 2c). No pitting was observed. Instead, consistent with the results seen in the other media, corrosion products are found deposited on the surface. The same result was observed when the sample was further corroded at more anodic potentials (0.4 V , images not shown). The O/Fe ratios of the two corroded samples, viz., 0.029 for SS304 and 0.015 for SS316, indicate that there are more oxygen atoms in the corrosion products seen on the SS304 surface than on the SS316 surface.

4. Conclusion

Corrosion of two stainless steels, SS304 and SS316, were studied in neutral, acidic and alkaline saline media using potentiodynamic polarization, scanning electron microscopy and energy dispersive X-ray spectroscopy. The results confirm the known result that SS316 has higher corrosion resistance than SS304. However, many significant additional findings have been brought out by a microscopic analysis of samples corroded at conditions determined by the potentiodynamic polarization experiments. The primary mechanism of SS304 corrosion is pitting, which is significantly minimized in SS316. For SS304 steels in neutral and alkaline media, small pits are initially formed which are then connected through intergranular corrosion. The pits then deepen. On the other hand, in acidic media,

SS304 forms large, chimney-like pits with intergranular corrosion linking the different pits through grain boundaries. Existing surface defects accelerate pitting and the overall corrosion rate. Corrosion products deposit better on SS316, resulting in more uniform corrosion than in SS304. This is particularly pronounced in neutral saline media, where SS316 does not show any evidence of significant local corrosion or passivation. This study shows that there is significant information that could be gleaned by supplementing the conventional potentiodynamic corrosion studies with SEM and EDX analyses.

5. Acknowledgment

The authors acknowledge the financial support of Amrita Vishwa Vidyapeetham. One of the authors (M.R.) acknowledges funds from the Ministry of Human Resource Development (FAST Scheme; F. No. 5-6/2013-TS.VII).

6. References

- [1] Fontana M 2017 *Corrosion Engineering* (New York: McGraw Hill)
- [2] Taji I *et al* 2015 *Corros. Sci.* **92** 301
- [3] Bertero E *et al* 2018 *Surf. Coat. Technol.* **349** 745
- [4] Lv Y *et al* 2018 *Prot. Met. Phys. Chem. Surf.* **54** 526
- [5] Sander G *et al* 2017 *J. Electrochem. Soc.* **164** C250
- [6] Ayu Arwati I G *et al* 2018 *IOP Conf. Ser.: Mater. Sci. Eng.* **343** 012016
- [7] Zeng L *et al* 2016 *Corros. Sci.* **111** 72
- [8] Karlsson J 2017 Pitting corrosion on stainless steel with and without passivation *Lund University* (<http://lup.lub.lu.se/student-papers/record/8903674>)
- [9] Hogg S M and Anderson B E 2018 *J. Acoust. Soc. Am.* **143** 1752
- [10] Ohasi K *et al* 2016 *NACE Int. Corros. Conf. Proc.* 7109
- [11] Gupta R K and Birbilis N 2015 *Corros. Sci.* **92** 1
- [12] Verma J and Taiwade R E 2017 *J. Manuf. Processes* **25** 134
- [13] Aoyama T *et al* 2017 *Corros. Sci.* **118** 217